ChemComm

COMMUNICATION

View Article Online
View Journal

Cite this: DOI: 10.1039/c4cc06559j

Received 20th August 2014,
Accepted 12th September 2014

DOI: 10.1039/c4cc06559j

www.rsc.org/chemcomm

Electrospun aggregation-induced emission active POSS-based porous copolymer films for detection of explosives†

Hui Zhou,[a] Qun Ye,[a] Wei Teng Neo,[a] Jing Song,[a] Hong Yan,[a] Yun Zong,[a] Ben Zhong Tang,*[b] T. S. Andy Hor[ac] and Jianwei Xu*[a]

Electrospun aggregation-induced emission (AIE)-active polyhedral oligomeric silsesquioxane (POSS)-based copolymer films exhibit an approximately 9-fold increase in response to explosive vapors compared to dense films although porous copolymer films have a thickness as high as 560 ± 60 nm.

In the past few decades, detection of explosives has become an internationally concerned issue for the anti-terrorism and homeland security. Most high explosives are nitro-substituted organic compounds. Typically, nitro-aromatics, such as 2,4,6-trinitrotoluene (TNT) and 2,4-dinitrotoluene (2,4-DNT), are the primary military explosives and also the principal components in the unexploded landmines worldwide.

Various analytical techniques have been used for the detection of explosives, such as chromatography using an ultraviolet absorption detector,[1] mass spectrometry,[2] Raman spectroscopy,[3] X-ray imaging,[4] thermal neutron analysis,[5] electrochemical assay,[6] and ion mobility spectroscopy,[7] which are always highly costly and difficult to use. Fluorescence based sensing has provided an alternative detection approach, which is highly sensitive, convenient and cost-effective. Fluorescent conjugated polymers have been applied as film sensing materials for the vapor detection of nitro compounds, because of their efficient exciton migration along the polymer chains.[8–10] However, the performance of most fluorescent sensory materials is limited by film thickness due to the fact that diffusion of analyte vapor in dense films is slow. A spin-coated conjugated polymer film achieves its optimum quenching efficiency towards TNT vapor with an ultra-thin film (*ca.* 2.5 nm) and experiences a sharp drop in quenching efficiency with film thicker than 25 nm.[11] To reduce the dependence of sensing performance on film thickness, a sensor based on a highly nanostructured film with a large surface-to-volume ratio, inherent high porosity, and easy accessibility of sensing materials is needed. On the other hand, aggregation-caused quenching (ACQ) of fluorescence is commonly observed in fluorescent conjugated polymers in the solid state, which has undermined their potential as solid state sensors or probes for explosive detection.[12]

Recently, aggregation induced emission (AIE) materials in the areas of optoelectronics[13] and sensory systems[14–16] have attracted increasing interest due to the absence of the ACQ effect. Fluorescence of the AIE active tetraphenylethene (TPE)-based polymers can be effectively quenched by nitroaromatics in solution.[17] However, the solid state sensing materials with AIE properties have been rarely used for vapor detection mainly due to the lack of suitable processable AIE active polymers. Herein, we report a feasible method to prepare AIE active copolymers using free radical copolymerization of polyhedral oligomeric silsesquioxane (POSS) acrylate and TPE-containing acrylate monomers. POSSs have been demonstrated as building blocks for the generation of porous materials through thermolysis,[18a] hydrosilylation,[18b] other coupling reactions,[18c] as well as free radical copolymerization with other monomers.[18d] Several porous materials derived from vinyl POSS exhibit Brunauer–Emmett–Teller (BET) surface areas as high as 700 $m^2\ g^{-1}$ and a maximum tunable mesopore volume of 2.0 $cm^3\ g^{-1}$.[18e–g] In this communication, POSS based AIE active copolymers show pronounced AIE effects in solution as well as in the solid state. Porous films fabricated from the copolymers by electrospinning showed high sensitivity and selectivity for the vapor detection of nitro-compounds.

The synthetic routes leading to acrylate monomers and polymers **P1-4** are shown in Scheme 1. The key intermediate 4-(1,2,2-triphenylvinyl)phenol (**1**) was prepared from 1-bromotriphenylethylene and 4-hydroxyphenylboronic acid *via* a Suzuki coupling reaction according to our previous work.[17f] Compound **1** reacted with 12-bromododecan-1-ol to produce precursor **2** with a reasonable yield of 86%, followed by treatment with acryloyl chloride in the presence of triethylamine in dry dichloromethane

---

[a] *Institute of Materials Research and Engineering, A*STAR (Agency for Science, Technology and Research), 3 Research Link, Singapore 117602, Republic of Singapore. E-mail: jw-xu@imre.a-star.edu.sg*
[b] *Department of Chemistry, The Hong Kong University of Science & Technology, Clear Water Bay, Kowloon, Hong Kong, China. E-mail: tangbenz@ust.hk*
[c] *Department of Chemistry, National University of Singapore, 3 Science Drive 3, Singapore 117543, Republic of Singapore*

† Electronic supplementary information (ESI) available. See DOI: 10.1039/c4cc06559j

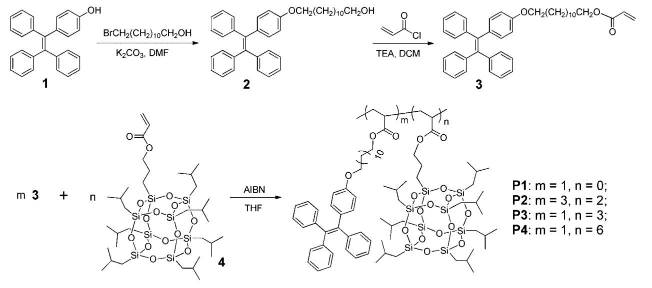

Scheme 1 Synthetic routes leading to monomer **3** and its corresponding polymers (**P1–P4**).

to afford monomer **3** with 95% yield. Finally, polymers **P1-4** were prepared from a mixture of monomer **3** and acryloisobutyl POSS (**4**) with different ratios by radical polymerization using AIBN as a radical initiator with 48–53% yields. Polymers **P1-4** were purified by re-precipitation twice in methanol to give white solids. They are soluble in most organic solvents such as tetrahydrofuran (THF), dichloromethane, chloroform and toluene. Polymers **P1-4** were structurally characterized by various spectroscopic methods and elemental analysis. The ratio of TPE to POSS was determined by ^{1}H NMR. Using **P2** as an example, the ^{1}H NMR spectrum of **P2** is illustrated in Fig. S1 in ESI.† The presence of signals at δ 7.03, 6.90 and 6.61 with an integration ratio of 15 : 2 : 2, which are assigned to the aromatic protons of the tetraphenylethene moiety, shows that the TPE moiety remained intact during the radical polymerization and purification process. The signal at δ 0.96 belongs to the protons of methyl groups in POSS (**4**). The presence of signals at δ 6.61 and 0.96 with an integration ratio of 1 : 14 suggests the ratio of monomer **3** to **4** be 3 : 2. The molecular weights of those polymers against polystyrene standards were determined by gel permeation chromatography (GPC) and the data are summarized in Table 1. The polymers show reasonable molecular weights of 18 800–32 200 Dalton with a relatively narrow polydispersity index of 1.36–1.68. Those polymers exhibited high thermal stability with decomposition temperatures ranging from 346 to 361 °C under nitrogen.

Electrohydrodynamic preparation is a convenient method used to produce polymer particles and fibers with diameters ranging from a few nanometers to several hundred micrometers.[19,20] The morphology of prepared substrates strongly depends on two main conditions including: (1) processing parameters, such as needle gauge, the flow rate, voltage, the distance between the needle and the collector and the type of collector; and (2) physicochemical properties of polymer solutions, such as molecular weight, solvent volatility, solution concentration and polymer–solvent interactions.[21] Generally, electrospinning the same polymer in different solvents could lead to substantially different morphologies of membranes.[21] In the present study, acetone–chloroform was selected as co-solvents because of the weak interaction between polymers and co-solvents as well as the low volatility of solvents which accelerates the drying process to prevent the formation of interconnected coarse fibers and webs. The electrohydrodynamic preparation of the POSS–MMA copolymer using acetone–chloroform co-solvent can successfully produce membranes with uniform fibers.[21a]

The films **F1–F8** were fabricated by electrospinning, drop-coating and spin-coating from different polymers, respectively. Concentration of the polymer in co-solvents was calculated in weight percent. At the beginning, we fabricated films using a polymer with a concentration of 2.0% in an acetone/chloroform mixture (1/1, v/v). SEM images of polymer films **F1-8** are shown in Fig. 1 and Fig. S2 (ESI†). The SEM results showed the morphological transition of polymers films from small crumpled particles with fibers (**F1** in Fig. 1), to particles (**F2** in Fig. S2, ESI†), to large crumpled particles with fibers (**F3** in Fig. S2, ESI†), to fibers (**F4** in Fig. 1). Films were fabricated using polymer **P4** at higher concentrations of 5.0% and 10.0%, and SEM images indicate the formation of particles with fibers under both conditions (**F5** and **F6** in Fig. S2, ESI†). It is observed that film **F4** exhibits a uniform porous fiber structure with the diameters of approximately 300 nm. Furthermore, films **F7** and **F8** were also fabricated by drop-coating and spin-coating using the solution of 2.0% **P4** in acetone/chloroform (1/1, v/v). In both cases, SEM images showed different morphologies from those obtained by electrohydrodynamic preparation. Film **F7** formed a porous structure with different sizes of holes ranging from 2 μm to 10 μm due to solvent evaporation. In contrast, film **F8** shows

Table 1 Properties of polymers **P1-4** and their corresponding films[a]

Polymer	Ratio of **3** : **4**	$M_w \times (10^{-3})$	M_w/M_n	T_d	T_g	T_m	Film	Thickness[b] (nm)
P1	3 : 0	32.2	1.68	356	49	—	**F1**	1400 ± 120
P2	3 : 2	21.6	1.37	346	23	—	**F2**	660 ± 60
P3	1 : 3	19.8	1.36	347	—	128	**F3**	650 ± 70
P4	1 : 6	18.8	1.36	349	—	141	**F4**	560 ± 60
P4							**F5**	740 ± 80
P4							**F6**	1580 ± 130
P4							**F7**	1300 ± 200
P4							**F8**	590 ± 30

[a] Not detected. [b] Experiments were performed in duplicate and mean values were taken. Films **F1–F6** are fabricated by electrospinning, and films **F7** and **F8** were fabricated by drop coating and spin coating, respectively.

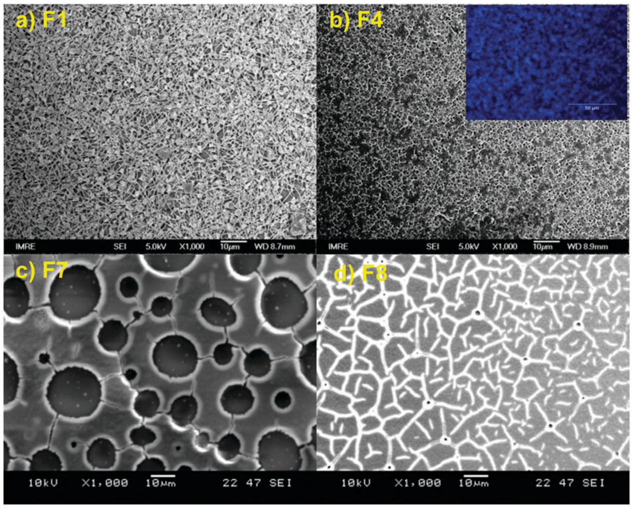

Fig. 1 SEM images of films: (a) **F1**, (b) **F4**, (c) **F7** and (d) **F8**, scale bar is 10 μm. See processing parameters in Table S1 (ESI†). The inserted photo in b is the fluorescence image of film **F2** taken under a fluorescence microscope with a 337 nm excitation; scale bar is 50 μm.

only a cracked surface. Thus, the morphology of polymer films with a uniform porous nanostructure can be easily achieved by judicious selection of suitable comonomers and their concentrations.

All polymers **P1-4** were non-emissive when dissolved in good solvents, such as THF, dichloromethane, chloroform and toluene. Taking **P4** solution in THF as an example (Fig. S3 in ESI†), the fluorescence became obvious when a large amount of H_2O ($>40\%$) was added into THF solution, indicating that TPE maintained its AIE activity after being incorporated into the polymer structure with POSS residues. However, these particles were much less stable than our reported AIE polymer nanoparticles.[17d] They tend to precipitate out even when stored at 4 °C for one day, which is likely caused by the hydrophobic nature of big POSS blocks in copolymers. Similar observations were seen for other formulations. For porous film **F1**, an obvious bathochromic/red shift of 11.5 nm was observed in the UV-Vis spectrum (Fig. 2a) in the aggregated state compared to its solution. This could be attributed to the enhanced planar conformation or aggregation of TPE units in the aggregated state. In contrast, for porous film **F4**, almost no bathochromic/red shift except a shoulder peak was found in the UV-vis spectra when compared to its solution, indicating the weak stacking of TPE residues in porous morphology structure, which was likely to be caused by the introduction of POSS into the polymer. The porous film **F4** displayed strong emission in the range from 375 to 600 nm with an emission maximum of 469 nm, and no shift was found compared to other polymers **P1–P3**.

The BET test displayed in Fig. 2b revealed that **P4** porous material produced by electrospinning had a BET surface area of 170 $m^2\ g^{-1}$, which was almost 57 fold greater than that of **P4** dense material produced by drop coating ($S_{BET} = 4\ m^2\ g^{-1}$). The significant increase in the BET surface area indicates the highly porous structure of film **F4** compared to film **F7**, which is in fact consistent with SEM observation. Typically, most porous materials with regular porous morphologies will be open and accessible to analyte molecules. In order to test the sensing ability, the copolymer films were investigated by exposing films to saturated DNT vapors at room temperature. As shown in Fig. 3a, fluorescence quenching was immediately observed by exposing porous film **F4** to saturated DNT vapor, and the fluorescence quenching of **F4** reached 52% in 30 s, 79% in 90 s and 90% in 4 min, respectively. In contrast, we also studied the fluorescence responsiveness ability of other copolymer films (Fig. 3b), and their quenching efficiencies upon exposure to DNT vapor for 4.0 min were less than 22%, which is much lower than 90% of film **F4**. Under the same conditions, the porous film **F1** without POSS residues showed a low quenching efficiency of 23%. Therefore, porous film **F4** displayed higher sensitivity to DNT vapor than other low porous films under the same conditions. Therefore, the sensitivity of the electrospun porous film is much higher than that of dense films. In conjunction with porous fibers created by electrospinning, the presence of POSS moieties in the copolymers enables the formation of porous structure, leading to an increase in total surface area and subsequently facilitating the diffusion of the gaseous analytes inside the polymer film and as a result improving its sensitivity.

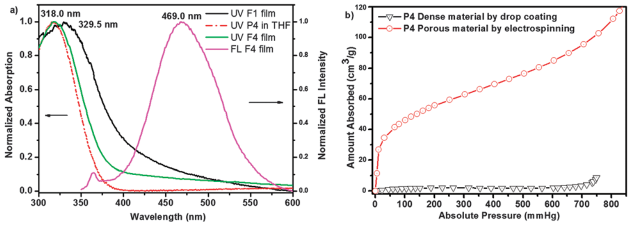

Fig. 2 (a) UV-Vis spectra of polymer **P4** in THF and porous films **F1** and **F4**, together with fluorescence spectra of porous film **F4**. (b) N_2 absorption isotherms at −196 °C for **P4** before and after electrospinning.

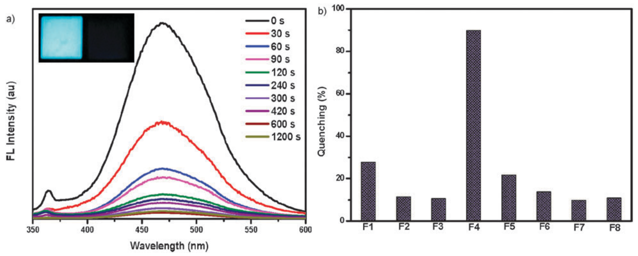

Fig. 3 (a) Fluorescence quenching of **F4** upon exposure to DNT saturated vapor, the insets display the photos of **F4** before and after exposure to DNT saturated vapor for 4 min under UV light (365 nm) illumination, at 25 °C. (b) Fluorescence quenching of films **F1–F8** in the presence of DNT saturated vapor for 4.0 min, at 25 °C.

The fluorescence response of the porous film **F4** to other nitro compound vapors was also investigated. As shown in Fig. 4a, the response of **F4** to TNT vapor was slower than that of DNT, and its fluorescence quenching reaches 15% in 60 s and 26% in 4.0 min, respectively. Finally, **F4** lost nearly 50% of fluorescent intensity after 20 min of exposure to saturated TNT vapor. Porous film **F4** showed higher sensing ability to DNT vapor probably due to its higher vapor concentration (*ca.* 100 ppb) relative to TNT (*ca.* 5 ppb). **F4**'s fluorescence was only quenched by 12% in 4.0 min for NT vapor, while almost no fluorescence response to highly volatile toluene vapor, demonstrating its good selectivity to explosive vapors. It is worth noting that the quenched fluorescence could be recovered by exposure to hydrazine vapor, and the recovered film still displayed sensing ability to explosives. After 5 off–on cycles, the florescence quenching towards to DNT vapor still remained around 78%, suggesting high stability and fluorescence reversibility of film **F4** (Fig. 4b).

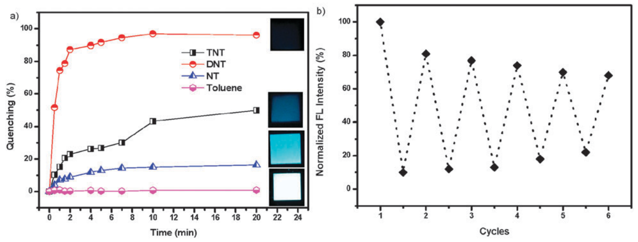

Fig. 4 (a) Time-dependent fluorescence quenching of porous film **F4** upon exposure to saturated vapor of TNT, DNT, NT and toluene, respectively. The insets display the photos of **F4** upon exposure to analyte saturated vapor under UV light (365 nm) illumination, 25 °C. (b) The fluorescence recovery of **F4** upon exposure to saturated vapor of DNT and hydrazine.

In summary, a new type of AIE active sensory material for explosive vapor detection has been developed based on a copolymer of acryloisobutyl POSS and TPE-containing acrylate monomers. The porous films were readily fabricated by electrospinning with a concentration of 2% in acetone–chloroform. Unlike fluorescent conjugated polymers, the porous AIE polymer films showed less dependence of fluorescence response to nitrocompounds on film thickness even though they have thickness as high as 560 ± 60 nm. This is due to the presence of POSS moieties, facilitating the formation of porous structures and subsequently leading to a large response to explosive vapors. Moreover, less dependence of response to nitro-compounds on film thickness avoids a tedious film fabrication method to control film thickness. Finally, electrospun AIE active films displayed remarkable fluorescence quenching sensitivity to TNT and DNT vapors compared to the corresponding dense films, making them promising for potential applications in the detection of explosives.

The authors would like to acknowledge the financial support (Grant No. 1321760011) from the Institute of Materials Research and Engineering (IMRE), Agency for Science, Technology and Research (A*STAR).

Notes and references

1 R. Hodyss and J. L. Beauchamp, *Anal. Chem.*, 2005, **77**, 3607–3610.

2 A. Popov, H. Chen, O. N. Kharybin, E. N. Nikolaev and R. G. Cooks, *Chem. Commun.*, 2005, 1953–1955.

3 J. M. Sylvia, J. A. Janni, J. D. Klein and K. M. Spencer, *Anal. Chem.*, 2000, **72**, 5834–5840.

4 S. F. Hallowell, *Talanta*, 2001, **54**, 447–458.

5 C. Vourvopoulos and P. C. Womble, *Talanta*, 2001, **54**, 459–468.

6 M. Krausa and K. Schorb, *J. Electroanal. Chem.*, 1999, **461**, 10–13.

7 (*a*) E. Wallis, T. M. Griffin, N. Popkie Jr., M. A. Eagan, R. F. McAtee, D. Vrazel and J. McKinly, *Proc. SPIE-Int. Soc. Opt. Eng.*, 2005, **5795**, 54–64; (*b*) G. A. Eiceman and J. A. Stone, *Anal. Chem.*, 2004, **76**, 390A–397A.

8 (*a*) S. Yamaguchi and T. M. Swager, *J. Am. Chem. Soc.*, 2001, **123**, 12087–12088; (*b*) S. Zahn and T. M. Swager, *Angew. Chem., Int. Ed.*, 2002, **41**, 4226–4230; (*c*) W. Thomas III, J. P. Amara, R. E. Bjork and T. M. Swager, *Chem. Commun.*, 2005, 4572–4574; (*d*) A. Narayanan, O. P. Varnavsky, T. M. Swager and T. Goodson III, *J. Phys. Chem. C*, 2008, **112**, 881–884; (*e*) S. Chen, Q. Zhang, J. Zhang, J. Gu and L. Zhang, *Sens. Actuators, B*, 2010, **149**, 155–160.

9 (*a*) A. Rose, Z. Zhu, C. F. Madigan, T. M. Swager and V. Bulovic, *Nature*, 2005, **434**, 876–879; (*b*) I. A. Levitsky, W. B. Euler, N. Tokranova and A. Rose, *Appl. Phys. Lett.*, 2007, **90**, 041904; (*c*) Y. Long, H. Chen, Y. Yang, H. Wang, Y. Yang, N. Li, K. Li, J. Pei and F. Liu, *Macromolecules*, 2009, **42**, 6501–6509.

10 J. T. Sarah and C. T. Willianm, *J. Mater. Chem.*, 2006, **16**, 2871–2883.

11 (*a*) J. S. Yang and T. M. Swager, *J. Am. Chem. Soc.*, 1998, **120**, 5321–5322; (*b*) J. S. Yang and T. M. Swager, *J. Am. Chem. Soc.*, 1998, **120**, 11864–11873; (*c*) H. Nie, Y. Zhao, M. Zhang, Y. Ma, M. Baumgarten and K. Müllen, *Chem. Commun.*, 2011, **47**, 1234–1236; (*d*) H. Nie, G. Sun, M. Zhang, M. Baumgarten and K. Müllen, *J. Mater. Chem.*, 2012, **22**, 2129–2132.

12 J. B. Birks, *Photophysics of Aromatic Molecules*, Wiley, London, 1970.

13 (*a*) Z. Zhao, S. Chen, J. W. Y. Lam, P. Lu, Y. Zhong, K. S. Wong, H. S. Kwok and B. Z. Tang, *Chem. Commun.*, 2010, **46**, 2221–2223; (*b*) V. S. Vyas and R. Rathore, *Chem. Commun.*, 2010, **46**, 1065–1067.

14 (*a*) J. Liu, Y. Zhong, P. Lu, Y. Hong, J. W. Y. Lam, M. Faisal, Y. Yu, K. S. Wong and B. Z. Tang, *Polym. Chem.*, 2010, **1**, 426–429; (*b*) T. Sanji, K. Shiraishi, M. Nakamura and M. Tanaka, *Chem. – Asian J.*, 2010, **5**, 817–824.

15 (*a*) M. Wang, G. Zhang, D. Zhang, D. Zhu and B. Z. Tang, *J. Mater. Chem.*, 2010, **20**, 1858; (*b*) S. J. Toal, K. A. Jones, D. Magde and W. C. Trogler, *J. Am. Chem. Soc.*, 2005, **127**, 11661; (*c*) Y. Hong, M. Haeussler, J. W. Y. Lam, Z. Li, K. K. Sin, Y. Dong, H. Tong, J. Liu, A. Qin, R. Renneberg and B. Z. Tang, *Chem. – Eur. J.*, 2008, **14**, 6428; (*d*) Y. Hong, H. Xiong, J. W. Y. Lam, M. Haessler, J. Liu, Y. Yu, Y. Zhong, H. H. Y. Sung, I. D. Williams, K. S. Wong and B. Z. Tang, *Chem. – Eur. J.*, 2010, **16**, 1232; (*e*) Y. Liu, Y. Tang, N. N. Barashkov, I. S. Irgibaeva, J. W. Y. Lam, R. Hu, D. Birimzhanova, Y. Yu and B. Z. Tang, *J. Am. Chem. Soc.*, 2010, **132**, 13951; (*f*) T. L. Andrew and T. M. Swager, *J. Am. Chem. Soc.*, 2007, **129**, 7254.

16 (*a*) S. Kim, H. E. Pudavar, A. Bonoiu and P. N. Prasad, *Adv. Mater.*, 2007, **19**, 3791; (*b*) J. Liu, J. W. Y. Lam and B. Z. Tang, *J. Inorg. Organomet. Polym. Mater.*, 2009, **19**, 249; (*c*) W. C. Wu, C. Y. Chen, Y. Tian, S. H. Jang, Y. Hong, Y. Liu, R. Hu, B. Z. Tang, Y. T. Lee, C. T. Chen, W. C. Chen and A. K. Y. Jen, *Adv. Funct. Mater.*, 2010, **20**, 1413; (*d*) M. Faisal, Y. Hong, J. Liu, Y. Yu, J. W. Y. Lam, A. Qin, P. Lu and B. Z. Tang, *Chem. – Eur. J.*, 2010, **16**, 4266; (*e*) F. Mahtab, Y. Yu, J. W. Y. Lam, J. Liu, B. Zhang, P. Lu, X. Zhang and B. Z. Tang, *Adv. Funct. Mater.*, 2011, **21**, 1733–1740.

17 (*a*) J. Liu, Y. Zhong, P. Lu, Y. Hong, J. W. Y. Lam, M. Faisal, Y. Yu, K. S. Wong and B. Z. Tang, *Polym. Chem.*, 2010, **1**, 426; (*b*) A. Qin, J. W. Y. Lam, L. Tang, C. K. W. Jim, H. Zhao, J. Sun and B. Z. Tang, *Macromolecules*, 2009, **42**, 1421–1424; (*c*) X.-M. Hu, Q. Chen, D. Zhou, J. Cao, Y.-J. He and B.-H. Han, *Polym. Chem.*, 2011, **2**, 1124–1128; (*d*) R. Hu, J. L. Maldonado, M. Rodriguez, C. Deng, C. K. W. Jim, J. W. Y. Lam, M. M. F. Yuen, G. Ramos-Ortiz and B. Z. Tang, *J. Mater. Chem.*, 2012, **22**, 232–240; (*e*) J. Li, J. Liu, J. W. Y. Lam and B. Z. Tang, *RSC Adv.*, 2013, **3**, 8193; (*f*) H. Zhou, J. Li, M. H. Chua, H. Yan, B. Z. Tang and J. Xu, *Polym. Chem.*, 2014, **5**, 5628–5637.

18 (*a*) M. F. Roll, J. W. Kampf, Y. Kim, E. Yi and R. M. Laine, *J. Am. Chem. Soc.*, 2010, **132**, 10171–10183; (*b*) L. Zhang, Q. Yang, H. Yang, J. Liu, H. Xin, B. Mezari, P. C. M. M. Magusin, H. C. L. Abbenhuis, R. A. v. Santen and C. Li, *J. Mater. Chem.*, 2008, **18**, 450–457; (*c*) Y. Wada, K. Iyoki, A. Sugawara-Narutaki, T. Okubo and A. Shimojima, *Chem. – Eur. J.*, 2013, **19**, 1700–1705; (*d*) J. J. Ou, Z. B. Zhang, H. Lin, J. Dong and H. F. Zou, *Anal. Chim. Acta*, 2013, **761**, 209–216; (*e*) I. Nischang, O. Bruggemann and I. Teasdale, *Angew. Chem., Int. Ed.*, 2011, **50**, 4592–4596; (*f*) F. Alves, P. Scholder and I. Nischang, *ACS Appl. Mater. Interfaces*, 2013, **5**, 2517–2526; (*g*) F. Alves and I. Nischange, *Chem. – Eur. J.*, 2013, **19**, 17310–17313.

19 (*a*) M. G. McKee, G. L. Wilkes and R. H. Colby, *Macromolecules*, 2004, **37**, 1760–1767; (*b*) G. Eda and S. Shivkumar, *J. Appl. Polym. Sci.*, 2007, **106**, 475–487; (*c*) S. L. Shenoy, W. D. Bates, H. L. Frisch and G. E. Wnek, *Polymer*, 2005, **46**, 3372–3384; (*d*) Y. Wu, J. A. MacKay, J. R. McDaniel, A. Chilkoti and R. L. Clark, *Biomacromolecules*, 2008, **10**, 19–24.

20 (*a*) D. H. Reneker, A. L. Yarin, H. Fong and S. Koombhongse, *J. Appl. Phys.*, 2000, **87**, 4531–4547; (*b*) S. V. Fridrikh, J. H. Yu, M. P. Brenner and G. C. Rutledge, *Phys. Rev. Lett.*, 2003, **90**, 144502; (*c*) M. G. McKee, T. Park, S. Unal, I. Yilgor and T. E. Long, *Polymer*, 2005, **46**, 2011–2015; (*d*) D. Li and Y. Xia, *Adv. Mater.*, 2004, **16**, 1151–1170.

21 (*a*) J. Liu, J. Fan, Z. Zhang, Q. Hu, T. Zeng and B. Li, *J. Colloid Interface Sci.*, 2013, **394**, 386–393; (*b*) A. Tuteja, W. Choi, J. M. Mabry, G. H. McKinley and R. E. Cohen, *Proc. Natl. Acad. Sci. U. S. A.*, 2008, **105**, 18200–18205; (*c*) V. A. Ganesh, A. S. Nair, H. K. Raut, T. T. Y. Tan, C. He, S. Ramakrishna and J. Xu, *J. Mater. Chem.*, 2012, **22**, 18479–18485; (*d*) A. Tuteja, W. Choi, M. Ma, J. M. Mabry, S. A. Mazzella, G. C. Rutledge, G. H. McKinley and R. E. Cohen, *Science*, 2007, **318**, 1618–1622.